JGP Journal of General Physiology

RESEARCH ARTICLE

A forward genetic screen identifies chaperone CNX-1 as a conserved biogenesis regulator of *ERG* K^+ channels

Xue Bai[1,2*], Kai Li[1*], Li Yao[1,2], Xin-Lei Kang[1], and Shi-Qing Cai[1]

The human ether-a-go-go–related gene (hERG) encodes a voltage-gated potassium channel that controls repolarization of cardiac action potentials. Accumulating evidence suggests that most disease-related hERG mutations reduce the function of the channel by disrupting protein biogenesis of the channel in the endoplasmic reticulum (ER). However, the molecular mechanism underlying the biogenesis of ERG K^+ channels is largely unknown. By forward genetic screening, we identified an ER-located chaperone CNX-1, the worm homologue of mammalian chaperone Calnexin, as a critical regulator for the protein biogenesis of UNC-103, the ERG-type K^+ channel in *Caenorhabditis elegans*. Loss-of-function mutations of *cnx-1* decreased the protein level and current density of the UNC-103 K^+ channel and suppressed the behavioral defects caused by a gain-of-function mutation in *unc-103*. Moreover, CNX-1 facilitated tetrameric assembly of UNC-103 channel subunits in a liposome-assisted cell-free translation system. Further studies showed that CNX-1 act in parallel to DNJ-1, another ER-located chaperone known to regulate maturation of UNC-103 channels, on controlling the protein biogenesis of UNC-103. Importantly, Calnexin interacted with hERG proteins in the ER in HEK293T cells. Deletion of *calnexin* reduced the expression and current densities of endogenous hERG K^+ channels in SH-SY5Y cells. Collectively, we reveal an evolutionarily conserved chaperone CNX-1/Calnexin controlling the biogenesis of ERG-type K^+ channels.

Introduction

The human ether-a-go-go–related gene (hERG) channel is a delayed rectifier voltage-gated K^+ channel that controls repolarization of action potentials in cardiomyocytes (Vandenberg et al., 2012). Dysfunction of hERG is associated with multiple human diseases, including long QT syndrome (LQTS; Curran et al., 1995; Sanguinetti et al., 1995; Trudeau et al., 1995), schizophrenia (Huffaker et al., 2009), epilepsy (Johnson et al., 2009), and multiple types of cancers (Pardo and Stühmer, 2014). Although most LQTS-related hERG mutations result in decreased surface expression of the channel (Harkcom and Abbott, 2010; Anderson et al., 2014), the molecular mechanism underlying maturation of hERG K^+ channel is not fully understood.

The sole *Caenorhabditis elegans* ERG-type K^+ channel, UNC-103, is homologous to hERG, with 70% amino acid identity in functionally important transmembrane domains and cyclic nucleotide–binding domain (Garcia and Sternberg, 2003; Li et al., 2017). Previous studies have demonstrated that worm homologues of hERG modifiers, KCR1, Hyperkinetic, and some J-proteins also affect the function of UNC-103 channels (Petersen et al., 2004; Li et al., 2017), suggesting the conserved regulatory mechanisms of ERG K^+ channels between *C. elegans* and humans. Given the convenience of genetic manipulation, *C. elegans* thus can be used as an animal model to identify novel cellular factors important for regulating ERG channel biogenesis.

In the previous work, through a genetic screen, we found DNJ-1, an ER-located chaperone, is critical for the biogenesis of the UNC-103 K^+ channel in *C. elegans* (Li et al., 2017). Although the expression level of UNC-103 was markedly decreased because of a loss-of-function (LOF) mutation in *dnj-1*, there were still remaining UNC-103 proteins in the *dnj-1* mutant worms, suggesting that other cell factors act independently of DNJ-1 to facilitate the biogenesis of ERG channels. In this study, by forward genetic screening, we identified CNX-1, the *C. elegans* homologue of mammalian chaperone Calnexin, as a critical factor for the biogenesis of ERG K^+ channels.

Calnexin, also known as CNX, IP90, or P88, is an ER-located chaperone with carbohydrate-binding activity (Ware et al., 1995; Schrag et al., 2001). A previous study has demonstrated that a trafficking defect in a LQTS-related mutant, $hERG^{N470D}$,

[1]Institute of Neuroscience and State Key Laboratory of Neuroscience, CAS Center for Excellence in Brain Science and Intelligence Technology, Chinese Academy of Sciences, Shanghai, China; [2]University of Chinese Academy of Sciences, Beijing, China.

*X. Bai and K. Li contributed equally to this paper; Correspondence to Shi-Qing Cai: sqcai@ion.ac.cn.

Table 1. **Summary of all worm strains used in this study**

Genotype	Strain	Description
unc-103(e1597)	CB1597	GOF worm mutant of *unc-103* (from CGC)
C. elegans wild isolate	N2	Bristol *C. elegans* (from CGC)
C. elegans wild isolate	CB4856	Hawaii *C. elegans* (from CGC)
cnx-1(yfh0017)	SQC0071	LOF worm mutant of *cnx-1*
cnx-1(yfh0018)	SQC0108	LOF worm mutant of *cnx-1*
cnx-1(yfh0019)	SQC0080	LOF worm mutant of *cnx-1*
cnx-1(yfh0020)	SQC0201	LOF worm mutant of *cnx-1*
unc-103(e1597);cnx-1(nr2010)	SQC0115	*unc-103(e1597)* crossed with *cnx-1(nr2010)*
unc-103^{A334T}	SQC0132	*yfhIx0132* (P*unc103*::*unc103^{A334T}*::GFP at 20 ng/µl)
unc-103^{A334T}; cnx-1(nr2010)	SQC0118	*unc-103^{A334T}* crossed with *cnx-1(nr2010)*
unc-103^{A334T}; dnj-1(yfh0001)	SQC0133	*unc-103^{A334T}* crossed with *dnj-1(yfh0001)*
unc-103^{A334T};cnx-1(nr2010); dnj-1(yfh0001)	SQC0119	*unc-103^{A334T}; dnj-1(yfh0001)* crossed with *cnx-1(nr2010)*
cnx-1(nr2010)	NS2932	LOF worm mutant of *cnx-1* (from CGC)
dnj-1(yfh0001)	SQC0001	LOF worm mutant of *dnj-1*
cnx-1(nr2010);dnj-1(yfh0001)	SQC0020	*cnx-1(nr2010)* crossed with *dnj-1(yfh0001)*
P*sp-12*::*sp12*::mCherry; P*cnx-1*::*cnx-1*::GFP	SQC2602	*yfhEx2602*(P*cnx-1*::*cnx-1*::GFP at 50 ng/µl, P*sp12*::*sp12*::mCherry at 50 ng/µl)
P*cnx-1*::mCherry;P*ver-3*::GFP	SQC2601	*yfhEx2601*(P*ver-3*::GFP at 50 ng/µl, P*cnx-1*::mCherry at 50 ng/µl)
P*unc-103*::mCherry; P*cnx-1*::GFP	SQC2600	*yfhEx2600* (P*cnx-1*::GFP at 50 ng/µl, P*unc-103*::mCherry at 50 ng/µl)
P*ver-3*::GFP(N2)	SQC0124	ALA neuron labeling in N2 (P*ver-3*::GFP at 30 ng/µl)
P*ver-3*::GFP[*cnx-1(nr2010)*]	SQC0125	ALA neuron labeling in *cnx-1(nr2010)* (P*ver-3*::GFP at 30 ng/µl)
P*ver-3*::GFP[*dnj-1(yfh0001)*]	SQC0126	ALA neuron labeling in *dnj-1(yfh0001)* (P*ver-3*::GFP at 30 ng/µl)
P*ver-3*::GFP[*cnx-1(nr2010); dnj-1(yfh0001)*]	SQC0127	ALA neuron labeling in *cnx-1(nr2010); dnj-1(yfh0001)* (P*ver-3*::GFP at 30 ng/µl)

CGC, Caenorhabditis Genetics Center.

is caused by a prolonged association with Calnexin (Gong et al., 2006). This result suggests that Calnexin may be involved in the biogenesis of hERG channels. However, the effect of Calnexin (or its worm homologue, CNX-1) on the biogenesis of ERG K^+ channels in vivo remains unclear. In this study, we demonstrated that Calnexin/CNX-1 interacted with the ERG channel and facilitated ERG channel biogenesis in the ER. The effect of CNX-1 on the biogenesis of the ERG channel involved its ability to promote tetrameric assembly of the channel subunits. Further experiments showed that the action of CNX-1 was independent of DNJ-1, suggesting that these two different types of chaperones facilitate the maturation of ERG channels via parallel pathways. Thus, we reveal a conserved role of CNX-1 in promoting ERG channel biogenesis.

Materials and methods

Worm strains and culture

OP50 bacteria-seeded nematode growth medium was used to cultivate worms at 20°C. N2, *unc-103(e1597)*, *cnx-1(nr2010)*, and CB4856 strains were obtained from the Caenorhabditis Genetics Center. The *dnj-1*(*yfh0001*) mutant was generated in our laboratory previously (Li et al., 2017). For detailed information of all the strains used in this study, please refer to Table 1.

Genetic screens and whole-genome sequencing

Synchronized L3-L4 stage *unc-103(e1597)* worms were used for mutagenesis. After treatment with 50 mM ethyl methanesulfonate for 4 h at room temperature, the F2 progenies of revertants (mutated worms that can move better and lay eggs) were selected. Hawaii CB4856 was crossed with the revertants to perform genetic mapping of the mutated genes (Davis et al., 2005). Genomic DNA of mutant worms was then prepared for whole-genome sequencing (Doitsidou et al., 2010). Genome sequencing was performed on an Illumina platform (HiSeq 2000/2500 or Hiseq X Ten), and all data were analyzed by CloudMap online software (https://usegalaxy.org). Rescue experiments of LOF alleles of *cnx-1* were performed by reexpressing wild-type CNX-1 proteins in *cnx-1* mutants.

Behavioral analyses of worms

Thrashing assays were performed as previously described (Petersen et al., 2004). In brief, young adult hermaphrodites were picked in M9 buffer and allowed to recover for 20 s. Thrashes were then counted for 30 s. A movement that the worm swings its head to the same side was counted as a thrash. For egg-laying, late L4 hermaphrodites were individually picked onto an OP50 seeded plate. After 30 h, the total number of the eggs and larvae on the plates was counted. The behavioral studies were not

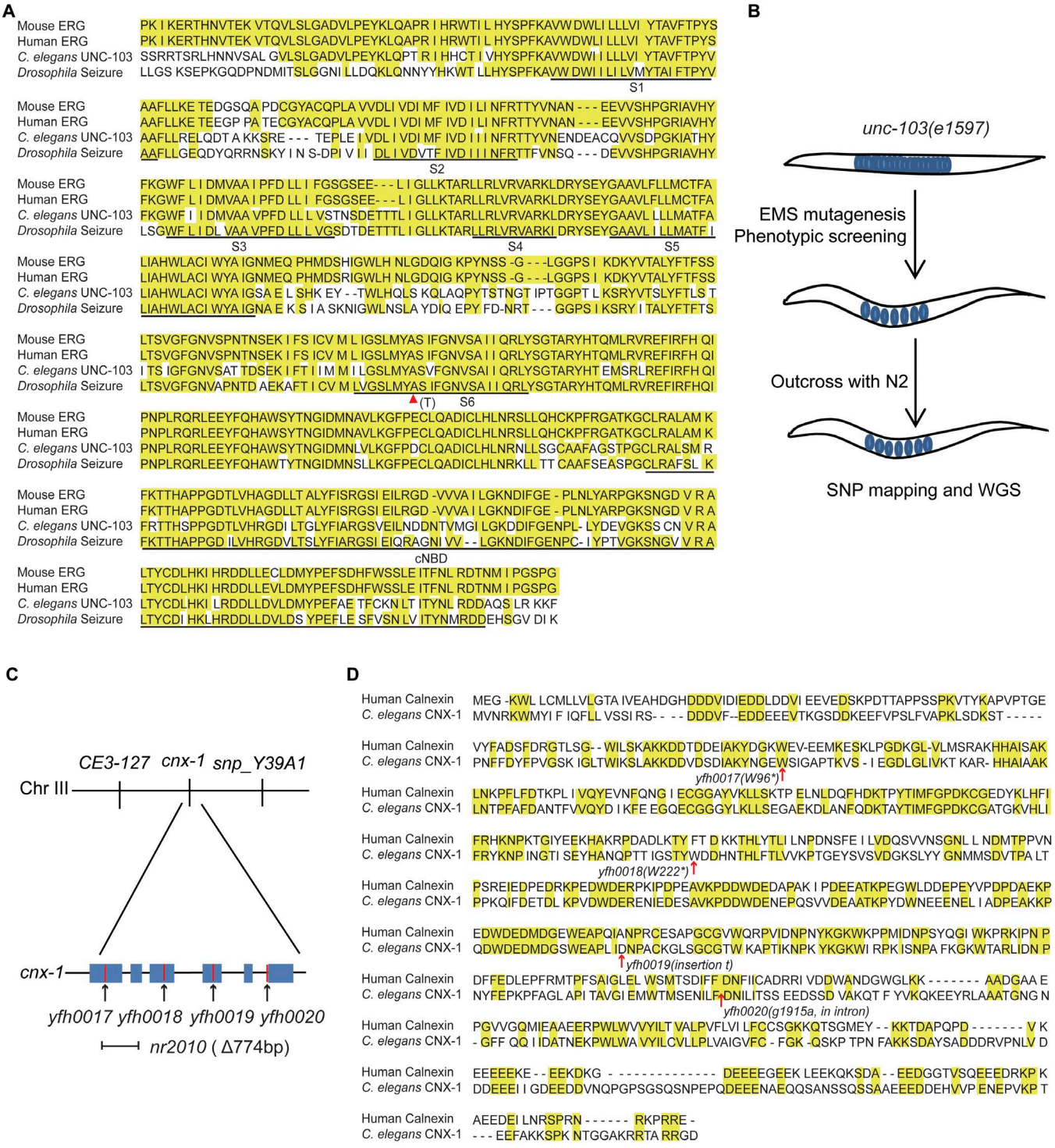

Figure 1. **A forward genetic screen identifies CNX-1 as a biogenesis regulator of UNC-103 K⁺ channel. (A)** Sequence alignment of transmembrane and cyclic nucleotide binding domains (cNBD) of mouse ERG, hERG, *C. elegans* UNC-103, and *Drosophila* Seizure channels. Identical amino acids are highlighted in yellow. Transmembrane and cyclic nucleotide binding domains are underlined. The triangle indicates the position of the GOF mutation in *unc-103.* **(B)** Schematic strategy of forward genetic screening. Mutagenesis was performed by treating *unc-103(e1597)* worms with ethyl methanesulfonate (EMS). EMS-induced mutants with recovery from behavioral defects were selected. SNP, single-nucleotide polymorphism; WGS, whole-genome sequencing. **(C)** Cloning of *cnx-1.* Chr III, chromosome III. Red lines indicate the mutated sites in exons and introns of the *cnx-1* gene. The deleted DNA fragment of *cnx-1* in *cnx-1(nr2010)* worms is indicated. **(D)** Sequence alignment of CNX-1 and its human homologue, Calnexin. Identical amino acids are shown in yellow. Arrows point to the mutated alleles in CNX-1.

Table 2. **Detailed information for different *cnx-1* alleles**

Gene	Strain	Allele	Effect	Gene change	Position
cnx-1	SQC0071	*yfh0017*	Stop codon	tGg/tAg	Exon 1
cnx-1	SQC0108	*yfh0018*	Stop codon	tgG/tgA	Exon 3
cnx-1	SQC0080	*yfh0019*	Insertion	Insertion t	Exon 4
cnx-1	SQC0201	*yfh0020*	Splicing site	G1915A	Last base pair in intron 5

conducted blind to genotypes, but two researchers independently did the experiments and obtained similar results.

Molecular biology and generation of transgenic worms

P_{cnx-1}*::gfp* and $P_{unc-103}$*::mCherry* were generated by inserting 2.2 kb *cnx-1* promoter and 4.3 kb *unc-103* promoter into the pPD95.75 vector, respectively, and then coinjected into N2 worms to analyze the expression pattern of *cnx-1*. ER marker *sp12* cDNA and *cnx-1* DNA were individually fused with the *cnx-1* promoter and then inserted into the pPD95.75 vector to generate P_{cnx-1}*::cnx-1::gfp* and P_{cnx-1}*::sp12::mcherry* plasmids. These two plasmids were coinjected into N2 worms to analyze the subcellular localization of CNX-1. P_{ver-3}*::gfp* was injected into N2, *cnx-1(nr2010)*, *dnj-1(yfh0001)*, or *cnx-1(nr2010);dnj-1(yfh0001)* worms to label the ALA neurons in these worm strains. For detailed information about these transgenic worms, please see Table 1.

calnexin cDNA was obtained from HEK293T cDNA library by PCR and inserted into the c-Myc-Pcs2+MT vector to generate the c-Myc-*calnexin* construct. The HA-hERG construct for expression in mammalian cells was generated previously (Li et al., 2017). *unc-103-gfp* and *cnx-1* cDNAs were individually inserted into the His-pEU expression vector for expressing proteins in the cell-free translation system.

All plasmids were verified by sequencing. Primers for cloning the *cnx-1* promoter were 5′-CATGCATGCCGGTTATTATTGGCGA-3′ (forward) and 5′-CGGGATCCGGTTACCTAAATTCA-3′ (reverse). Primers for cloning *cnx-1* DNA were 5′-CGGGATCCATGGTGA ACCGGAA-3′ (forward) and 5′-GGGGTACCCCATCCCCTCGGCG-3′ (reverse). Primers for cloning *sp12* cDNA were 5′-CGGGATCCATGG ACGGAATGATTGCA-3′ (forward) and 5′-GGGGTACCTTTCGTCTTC TTTGTCTC-3′ (reverse). Primers for cloning *calnexin* cDNA were 5′-CGGAATTCAATGGAAGGGAAGTGGTTGCTG-3′ (forward) and 5′-CCGCTCGAGTCACTCTCTTCGTGGCTTTCT-3′ (reverse).

Cell-free expression

Cell-free syntheses were performed using the WEPRO7240H Expression kit (Cell Free Sciences) according to protocol described previously (Li et al., 2017), with slight modifications. In brief, 2 µg purified plasmid DNA was transcribed at 37°C for 6 h. Translation reactions were then performed in the presence of 4 mg/ml soybean liposomes (Avanti Polar Lipids) at 25°C for 20 h. The proteoliposomes were solubilized by 1% m/v dodecylmaltoside (Sigma) and subjected to native PAGE electrophoresis.

C. elegans neuron culture

Primary cultures of *C. elegans* embryos were performed according to protocol described previously (Strange et al., 2007). In brief, worm embryos were isolated from adult hermaphrodites. After removal of the worm eggshells by enzymatic digestion, cells were dissociated and plated onto the dishes precoated with peanut lectin (Sigma). Whole-cell patch clamp was performed 4–6 d after seeding.

Immunocytochemistry

HEK293T cells were fixed with 4% paraformaldehyde (Sigma-Aldrich) for 30 min at room temperature, followed by permeabilization with 0.25% Triton X-100. After washing three times with PBS buffer, cells were blocked with 1% BSA for 1 h at room temperature. The primary antibodies used in this experiment were anti-HA (1:1,000, Roche) and anti-Calnexin (1:1,000; Abcam). The secondary antibodies were Alexa Fluor 488 (green) or Alexa Fluor 594 (red)–conjugated antibodies.

Western blot and immunoprecipitation

HEK293T and SH-SY5Y cells were cultured in Dulbecco's modified Eagle's medium (Gibco) with 10% FBS (Gibco), and 1% penicillin/streptomycin (Gibco) at 37°C in a 5% CO_2 incubator. Lipofectamine 2000 (Invitrogen) was used for plasmid transfection. The components of cell lysis buffer were 1% NP-40, 150 mM NaCl, 1 mM NaF, 50 mM Tris, pH 7.6, and protease inhibitor mixture (Roche). Cells were lysed in lysis buffer at 4°C for 1 h. After centrifugation at 4°C at 12,000 *g* for 10 min, the supernatants were collected and incubated with the primary antibody at 4°C for 3.5 h. The immune complexes were associated with protein A/G agarose beads (Santa Cruz) at 4°C for 2.5 h. The beads were then washed six times and boiled for 5 min. The Western blot analyses of UNC-103 protein levels were not conducted blind to genotypes, but two researchers independently did the experiments and obtained similar results. The following antibodies were used in these experiments: rabbit anti-hERG (Millipore), rabbit anti–c-Myc (Sigma), rat anti-HA (Roche), mouse anti-tubulin (Sigma), mouse anti-GFP (Abmart), and rabbit anti-actin (Abmart).

RNA interference

For knockdown experiments by siRNA, siRNAs were first transfected into HEK293T cells and then cotransfected with HA-hERG plasmid 16 h later. The scrambled (control) siRNA and human *calnexin* siRNA were purchased from Genepharma. The sequence of the control siRNA was 5′-UUCUCCGAACGUGUCACGUTT-3′. Two siRNAs corresponding to the human *calnexin* coding sequences (5′-AAGACGATACCGATGATGAAA-3′ and 5′-AATGTGGTGGTG CCTATGTGA-3′) were used according to the previous study (Swanton et al., 2003).

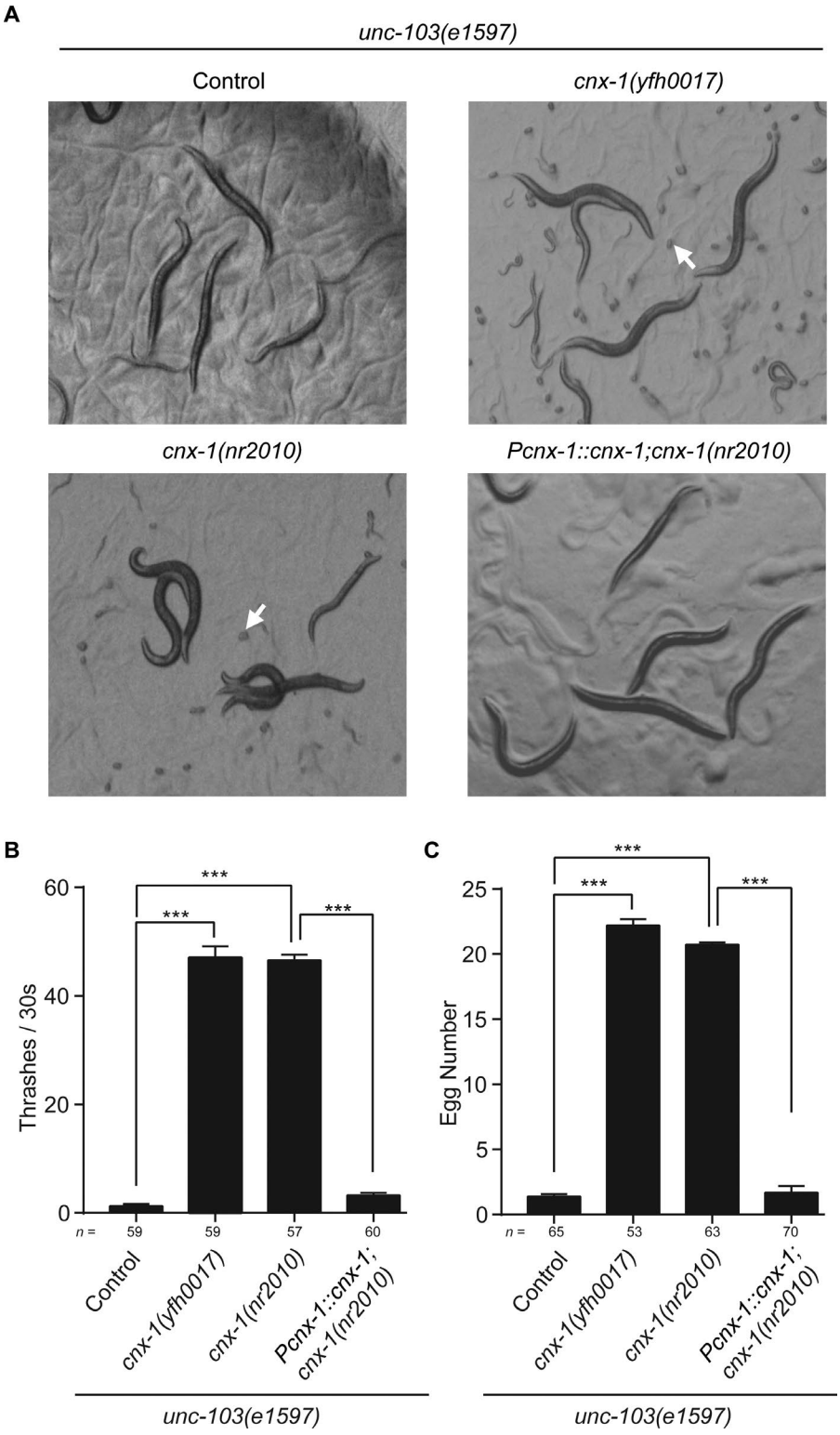

Figure 2. **Mutations in *cnx-1* suppress the behavioral defects of *unc-103(e1597)*.** **(A)** Images of *unc-103(e1597)* (control), *unc-103(e1597);cnx-1(yfh0017)*, *unc-103(e1597);cnx-1(nr2010)*, and P_{cnx-1}::*cnx-1;unc-103(e1597);cnx-1(nr2010)* worms. Arrows indicate eggs. P_{cnx-1}::*cnx-1;unc-103(e1597);cnx-1(nr2010)* worms were generated by reexpressing wild-type *cnx-1* in *unc-103(e1597);cnx-1(nr2010)* worms. **(B and C)** Quantification of thrashing (B) and egg-laying (C) behaviors in *unc-103(e1597)*, *unc-103(e1597);cnx-1(yfh0017)*, *unc-103(e1597);cnx-1(nr2010)*, and P_{cnx-1}::*cnx-1;unc-103(e1597);cnx-1(nr2010)* worms. The number of worms used in these experiments is indicated just below each column. All experiments were performed three times. Data shown are mean ± SEM. ***, $P < 0.001$ (*t* test).

Clustered regularly interspace short palindromic repeats (CRISPR)-Cas9–mediated genome editing

SH-SY5Y cell line with deletion of *calnexin* was generated by CRISPR-Cas9–mediated genome editing according to the standard protocol described previously (Ran et al., 2013). We used four sgRNAs targeting four loci of *calnexin* to induce DNA double strand breaks. sgRNAs were individually cloned into the CRISPR vector. The sequences of sgRNAs were 5′-GCTTGGAACTGCTATTGTTG-3′, 5′-CCTCTTCAATGACATCGTCA-3′, 5′-TTTGACAGAGGAACTCTGTC-3′, and 5′-TATACTTCCCCTGTTGGAAC-3′. *Calnexin*$^{-/-}$ cells were verified by DNA sequencing (the PCR primers were forward, 5′-GTTTTAACGGGTACCCCCTGT-3′ and reverse, 5′-AGAGTGGGGGAAAGAA-3′), followed by Western blot analysis using Calnexin antibody (Abcam) to detect Calnexin proteins in the cells.

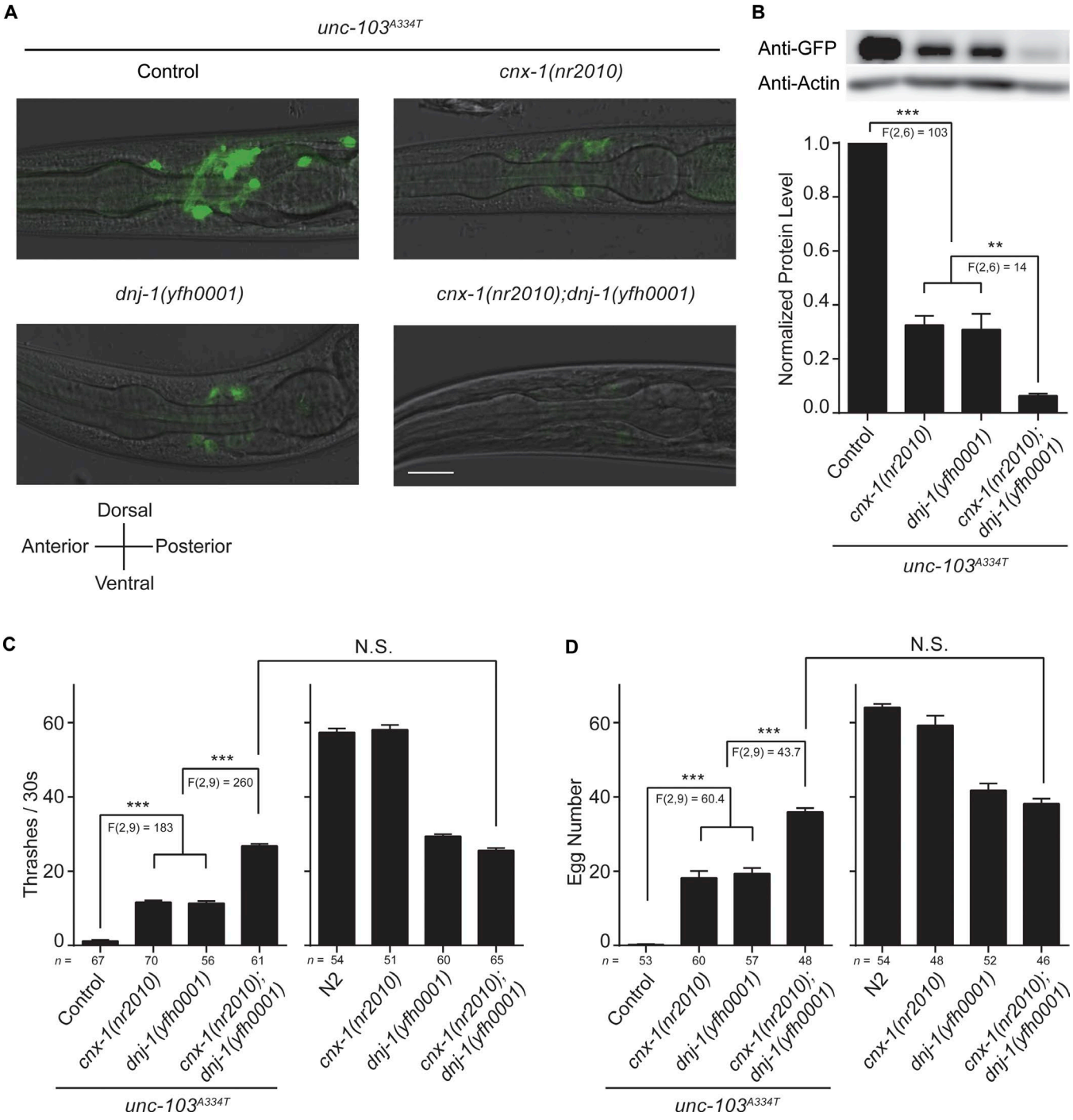

Figure 3. **CNX-1 regulates the biogenesis of UNC-103. (A and B)** Fluorescent images (A) and Western blot analysis (B) of the expression of UNC-103::GFP proteins in *unc-103*^{A334T} (control), *unc-103*^{A334T}*;dnj-1(yfh0001)*, *unc-103*^{A334T}*;cnx-1(nr2010)*, and *unc-103*^{A334T}*;dnj-1(yfh0001);cnx-1(nr2010)* worms. The worms' orientation depiction is shown in the bottom left. Bar, 15 µm. UNC-103::GFP fusion proteins were detected by anti–GFP antibodies. **(C and D)** Thrashing (C) and egg-laying (D) behaviors in worms. The number of worms used in these experiments is indicated just below each column. All experiments were performed at least three times. Data shown are mean ± SEM. N.S., not significant (*t* test). **, P < 0.01; ***, P < 0.001 (ANOVA with Dunnett's test). Degrees of freedom and outcome of post hoc testing are indicated below the significance asterisks.

Electrophysiology

The K^+ currents of ERG channels in cells were recorded by whole-cell patch clamp as described previously (Li et al., 2017). Pipette resistances were 5 MΩ for recording in HEK293T cells and SH-SY5Y cells. Pipette resistances were 15 MΩ for recording in *C. elegans* ALA neurons. The pipette solution for patch clamp in HEK293T cells contained (in mM) 100 KCl, 1 $MgCl_2$, 1 $CaCl_2$, 10 EGTA, and 10 HEPES, pH 7.5 (with KOH); and bath solution for HEK293T cells contained (in mM) 4 KCl, 100 NaCl, 10 HEPES, 1 $MgCl_2$, and 1.8 $CaCl_2$, pH 7.5 (with NaOH). For SH-SY5Y cells, the pipette solution was (in mM) KCl 135, $MgCl_2$ 1, and EGTA 10, HEPES 10, pH 7.2 (with KOH); and bath solution was (in mM)

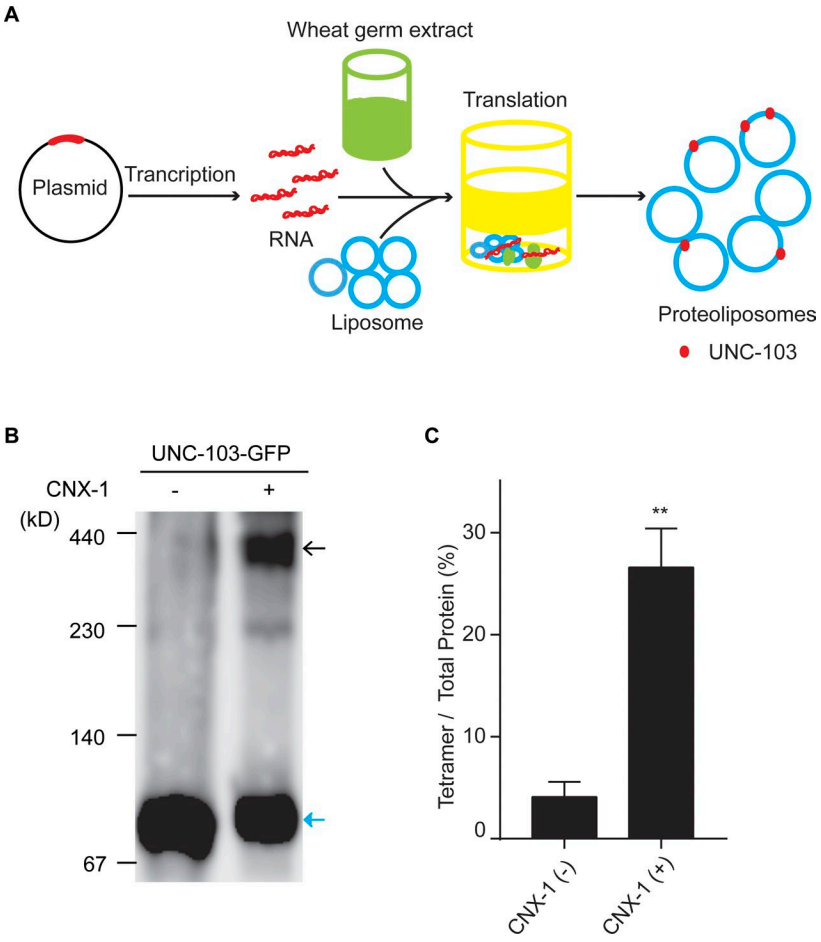

Figure 4. **CNX-1 facilitates tetrameric assembly of UNC-103 channel subunits. (A)** Schematic illustration of protein translation in wheat germ cell-free extracts with liposomes. **(B)** Effect of CNX-1 on the oligomerization of UNC-103::GFP proteins. Monomeric and tetrameric UNC-103::GFP proteins are indicated by blue and black arrows, respectively. UNC-103::GFP proteins were detected using anti–GFP antibody. **(C)** Quantification of assembly efficiency. The efficiency of UNC-103 assembly is calculated as the ratio of the UNC-103 tetramers to the total UNC-103 proteins (UNC-103 tetramers plus monomers). The experiment was performed three times. Data shown are mean ± SEM. **, $P < 0.01$ (*t* test).

KCl 5, NaCl 130, glucose 10, $MgCl_2$ 1, and $CaCl_2$ 2, HEPES 10, pH 7.4 (with NaOH). For *C. elegans* ALA neurons, the bath solution contained (in mM) 5 KCl, 145 NaCl, 1 $CaCl_2$, 5 $MgCl_2$, 10 HEPES/NaOH, pH 7.5, and 20 d-glucose. The pipette solution contained (in mM) 18 KCl, 125 potassium gluconate, 0.7 $CaCl_2$, 2 $MgCl_2$, 10 EGTA/KOH, 2 Mg-ATP, and 10 HEPES/KOH, pH 7.5. ERG K^+ currents were isolated by application of 1 µM E-4031 in the pipette solution.

Statistical analyses

The band intensities in immunoblots were determined by ImageJ software. The amplitudes of K^+ currents and the membrane capacitances of the recorded cells were measured using Clampfit software (version 10.4; Molecular Devices). Peak currents and steady-state currents at each voltage step were used for statistical analyses. Graphing and statistical comparisons were performed with GraphPad 7.0 software using either ANOVA or *t* test as specified in the figure legends.

Results

LOF mutations of *cnx-1* suppress the behavioral defects in *unc-103(GOF)* worms

The *C. elegans* ERG K^+ channel UNC-103 showed homology with the hERG channel (Fig. 1 A). *unc-103(e1597)* mutant worms exhibit severe defects in locomotion and egg-laying caused by a gain-of-function (GOF) mutation (A334T) in the S6 transmembrane domain of UNC-103 (Garcia and Sternberg, 2003; Reiner et al., 2006). The mutation is a GOF allele that alters the channel activation potential to a more negative value (Petersen et al., 2004) and inhibits the excitability of the cell (Collins and Koelle, 2013). We thus hypothesized that inhibition of the function of UNC-103 will alleviate the behavioral defects in *unc-103(e1597)* mutant worms. To identify novel regulators of ERG K^+ channels, we performed a forward genetic screen for suppressors of the behavioral defects of *unc-103(e1597)* worms. The screening strategy is depicted in Fig. 1 B.

From a screen of 14,000 haploid genomes, we isolated eight mutants with reverted phenotypes. Four of the isolated mutants were mapped to one gene, *cnx-1* (*ZK632.6*), which encodes a chaperone protein showing homology with mammalian Calnexin, through single-nucleotide polymorphism–based mapping (Fig. 1, C and D). Molecular lesions were identified in all the four *cnx-1* alleles through DNA sequencing (Fig. 1 D and Table 2). As shown in Fig. 2 (A–C), the behavioral defects in locomotion (quantified by thrashing) and egg laying (quantified by egg numbers) found in *unc-103(e1597)* worms were partially prevented by a LOF mutation or a deletion allele (*nr2010*) of the *cnx-1* gene. We then performed rescue experiments by reexpressing the wild-type CNX-1 with the driver of its own promoter in *unc-103(e1597);cnx-1(nr2010)* worms and found that reintroduction of the wild-type CNX-1 could reinstate the behavioral defects of *unc-103(e1597)* (Fig. 2, B and C), demonstrating that the lack of the CNX-1 protein, but not

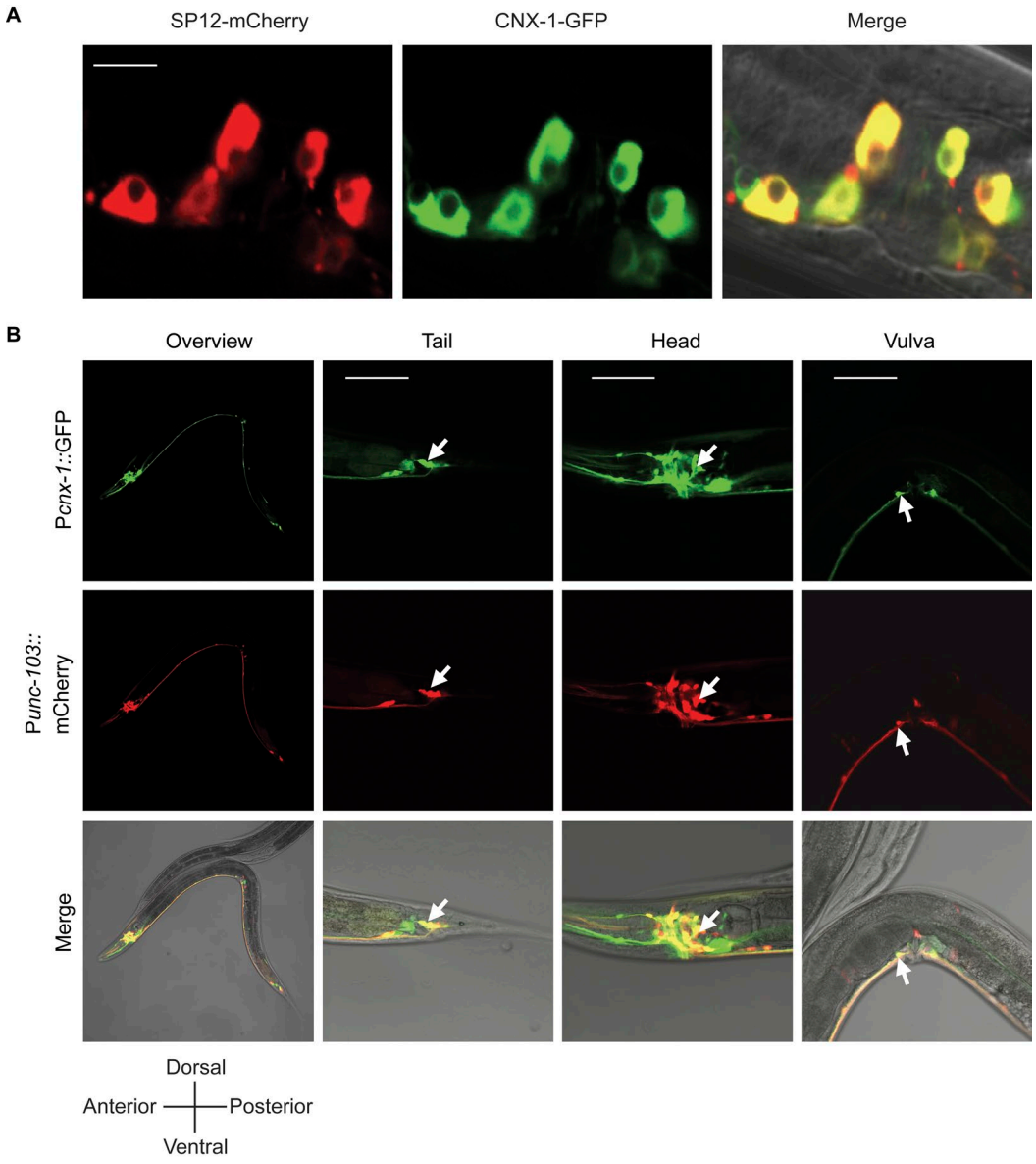

Figure 5. **Expression patterns of CNX-1. (A)** Subcellular localization of CNX-1. Expression of CNX-1-GFP and SP12-mCherry (an ER marker) were both driven by the *cnx-1* promoter. Bar, 5 µm. **(B)** Representative fluorescent images of wild-type N2 worms expressing *Pcnx-1*::GFP and *Punc-103*::mCherry reporters. Bars, 20 µm. Arrows indicate neurons. The worm's orientation depiction is shown in the bottom left.

other mutations in the genetic background, is responsible for the observed phenotypes. Together, these results suggest that CNX-1 is essential for the function of the UNC-103 K^+ channel in *C. elegans*.

CNX-1 is required for UNC-103 biogenesis

Our previous study generated a transgenic strain (named *unc-103^{A334T}*) expressing the GFP fused *unc-103* with the same GOF mutation found in *unc-103(e1597)* worms (Li et al., 2017). Like *unc-103(e1597)*, the transgenic worm exhibited severe defects in locomotion and egg laying, indicating that expression of UNC-103^{A334T}::GFP was sufficient to induce functional defects caused by the UNC-103 mutation, presumably by causing membrane hyperpolarization after its delivery to the plasma membrane.

To test whether CNX-1 regulates UNC-103 protein biogenesis, we crossed *unc-103^{A334T}* transgenic worms with the *cnx-1(nr2010)* worms to obtain the *unc-103^{A334T};cnx-1(nr2010)* strain. We found that the expression level of UNC-103^{A334T}::GFP was significantly reduced in *unc-103^{A334T};cnx-1(nr2010)* worms compared with *unc-103^{A334T}* worms (Fig. 3, A and B). Furthermore, the behavioral defects of *unc-103^{A334T}* transgenic worms were significantly suppressed by the LOF mutation in *cnx-1* (Fig. 3, C and D, left). Thus, these results suggest that CNX-1 is required for the protein biogenesis of UNC-103 in *C. elegans*.

Formation of functional K^+ channels requires channel subunits assembly, an important biogenic step occurring in the ER (Doyle et al., 1998; Isacoff et al., 2013). We then explored whether CNX-1 plays a role in the tetrameric assembly of UNC-103 channel subunits using a wheat germ cell-free system to synthesize proteins in vitro (Fig. 4 A). UNC-103 and CNX-1 were expressed in the cell-free extracts with liposomes that provide a hydrophobic

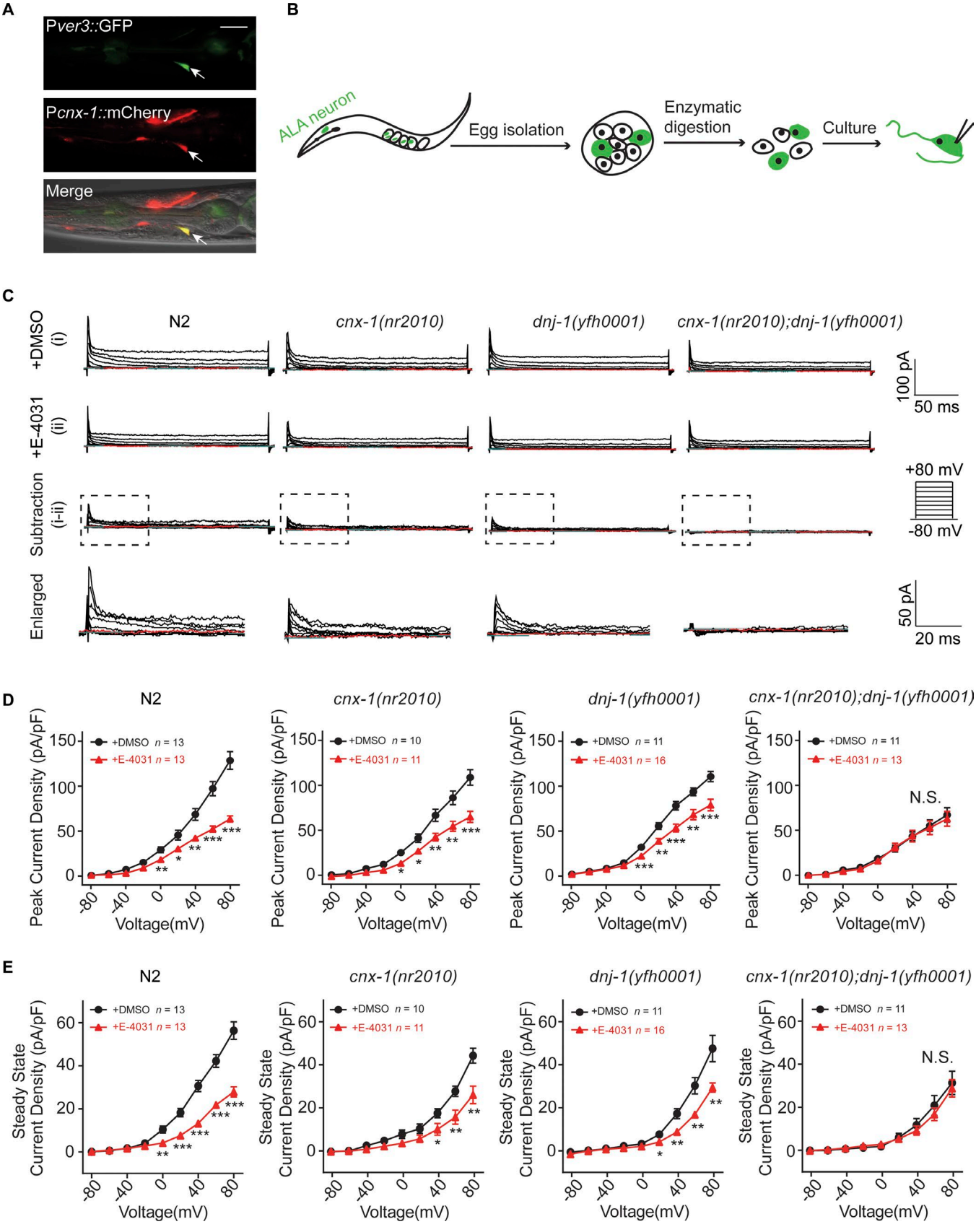

Figure 6. **CNX-1 regulates UNC-103 K⁺ currents. (A)** Fluorescent images of transgenic worms expressing *Pver-3*::GFP and *Pcnx-1*::mCherry. Arrows indicate ALA neurons. Bar, 10 µm. **(B)** Schematic illustration of primary culture of *C. elegans* neurons for electrophysiological recordings. Whole-cell patch clamp was performed 4–6 d after seeding *C. elegans* embryonic cells. **(C)** Representative whole-cell K⁺ currents recorded in *C. elegans* ALA neurons with or without the

environment to help the folding and assembly of these membrane proteins (Goren et al., 2009). We found that in vitro–synthesized UNC-103 existed as monomers, whereas part of the UNC-103 proteins appeared as tetramers upon coexpression with CNX-1 (Fig. 4, B and C), indicating that CNX-1 promotes tetrameric assembly of UNC-103 channel subunits in vitro.

The effects of CNX-1 and DNJ-1 on UNC-103 protein biogenesis are additive

Previous studies have demonstrated that DNJ-1, another ER-located chaperone protein, is critical for the biogenesis of the UNC-103 K^+ channel (Li et al., 2017). We then asked whether CNX-1 and DNJ-1 regulate the biogenesis of UNC-103 via the same pathway. We found that the expression level of UNC-103^{A334T}::GFP was markedly reduced by introducing either null mutations in *cnx-1* or *dnj-1* and almost abolished by introducing both the *cnx-1* and *dnj-1* mutations (Fig. 3, A and B). The locomotion and egg-laying defects found in *unc-103^{A334T}* worms could be partially prevented by null mutations in either *cnx-1* or *dnj-1* and further prevented by a combination of *cnx-1* and *dnj-1* null mutations (Fig. 3, C and D, left). Notably, locomotion and egg production in *cnx-1(nr2010);dnj-1(yfh0001)* worms were not significantly different from those in *unc-103^{A334T};cnx-1(nr2010);dnj-1(yfh0001)* worms, suggesting that the combination of *cnx-1* and *dnj-1* null mutations fully suppressed the locomotion and egg-laying defects caused by the GOF mutation in UNC-103. Thus, the effects of CNX-1 and DNJ-1 on UNC-103 channel biogenesis are additive.

CNX-1 regulates the function of endogenous UNC-103 K^+ channels

To determine the subcellular localization of CNX-1 proteins, we fused GFP and mCherry to the C termini of CNX-1 and the ER marker protein SP12, respectively. We found that CNX-1 was colocalized with SP12 in *C. elegans* neurons (Fig. 5 A), indicating that CNX-1 is an ER-located protein. Further study showed that *cnx-1* promoter–driven GFP was ubiquitously expressed in large numbers of neurons in the tail, head, and vulva (Fig. 5 B) and colocalized with *unc-103* promoter–driven mCherry in many neurons (Fig. 5 B), suggesting that CNX-1 and UNC-103 may interact with each other in vivo.

Furthermore, *cnx-1* promoter–driven mCherry proteins were colocalized with the ALA-specific *ver-3* promoter–driven GFP, suggesting that CNX-1 was expressed in ALA neurons (Fig. 6 A). To investigate whether CNX-1 regulates endogenous UNC-103 K^+ channels, we examined the effect of CNX-1 on UNC-103 function in ALA neurons, where UNC-103 is expressed (Li et al., 2017). We recorded outward K^+ currents in cultured *C. elegans* ALA neurons, which were labeled by ALA-specific *ver-3* promoter–driven GFP (Fig. 6 B). Endogenous UNC-103 currents were isolated by E-4031, an ERG K^+ channel–specific blocker (Fig. 6 C). Compared with those in wild-type N2 worms, E-4031–sensitive currents of ALA neurons in *cnx-1(nr2010)* worms were reduced (Fig. 6, D and E), indicating that CNX-1 regulates endogenous UNC-103 K^+ channels in *C. elegans*. Furthermore, we found that both *dnj-1* and *cnx-1* mutant worms showed decreased UNC-103 currents (isolated by E-4031) in ALA neurons (Fig. 6, D and E), whereas the UNC-103 currents in *cnx-1(nr2010);dnj-1(yfh0001)* double-mutant worms were eliminated (Fig. 6, D and E). These results further suggest that CNX-1 and DNJ-1 regulate the function of the UNC-103 K^+ channel independent of each other.

Calnexin regulates the biogenesis of hERG K^+ channel in mammalian cells

C. elegans CNX-1 is homologous with mammalian protein Calnexin. We thus investigated whether Calnexin plays an evolutionarily conserved role in regulating the biogenesis of hERG channels. Immunostaining in HEK293T cells showed that hERG proteins distributed in both the cell surface and the ER (Fig.7 A). Consistent with the previous studies (Zhou et al., 1998; Anderson et al., 2006), we found two forms of hERG proteins corresponding to ER (~135 kD) and post-ER (~155 kD) forms with different extents of glycosylation (Fig. 7 B). Coimmunoprecipitation assays showed that Calnexin only interacted with the ER-residing form of hERG proteins (Fig. 7 B), suggesting that Calnexin interacts with hERG proteins in the ER.

We next investigated whether hERG K^+ channels could be regulated by Calnexin. In HEK293T cells expressing hERG proteins, down-regulation of *calnexin* by siRNA markedly decreased the protein level (Fig. 7 C) and current density (Fig. 7 D) of hERG K^+ channels. In human neuroblastoma SH-SY5Y cells that endogenously express hERG K^+ channels, deletion of *calnexin* by CRISPR-Cas9–mediated genome editing significantly decreased the endogenous hERG protein level (Fig. 7 E). Furthermore, the deactivating inward currents, which are mainly conducted by hERG channels (Meyer and Heinemann, 1998; Taglialatela et al., 1998; Li et al., 2017), were significantly reduced in *calnexin*$^{-/-}$ SH-SY5Y cells compared with wild-type SH-SY5Y cells (Fig. 7 F). Collectively, these findings suggest that Calnexin is essential for the protein biogenesis of native hERG channels in human cells.

Discussion

In this study, through forward genetic screen in *C. elegans*, we found that CNX-1 is a critical regulator of the UNC-103 K^+ channel. LOF mutations of *cnx-1* resulted in a reduced protein level

ERG channel–specific blocker E-4031 (1 µM) in the bath solution. The voltage protocol is shown on the right. Traces shown are the mean of all recordings. UNC-103–elicited K^+ currents in ALA neurons are shown by mean outward K^+ currents (i) subtracting mean retained currents (ii) after treatment with the ERG channel–specific blocker E-4031. The magnified currents of the corresponding dotted boxes are shown. **(D)** Peak current density of voltage-gated outward K^+ currents at different membrane potentials in ALA neurons in the absence (black line) and presence (red line) of 1 µM E-4031 in the pipette solution. **(E)** Steady-state current density of voltage-gated outward K^+ currents at different membrane potentials in ALA neurons in the absence (black line) and presence (red line) of 1 µM E-4031 in the pipette solution. For D and E, the cell numbers used for analyses are indicated. Data shown are mean ± SEM. N.S., not significant; *, $P < 0.05$; **, $P < 0.01$; ***, $P < 0.001$ (*t* test).

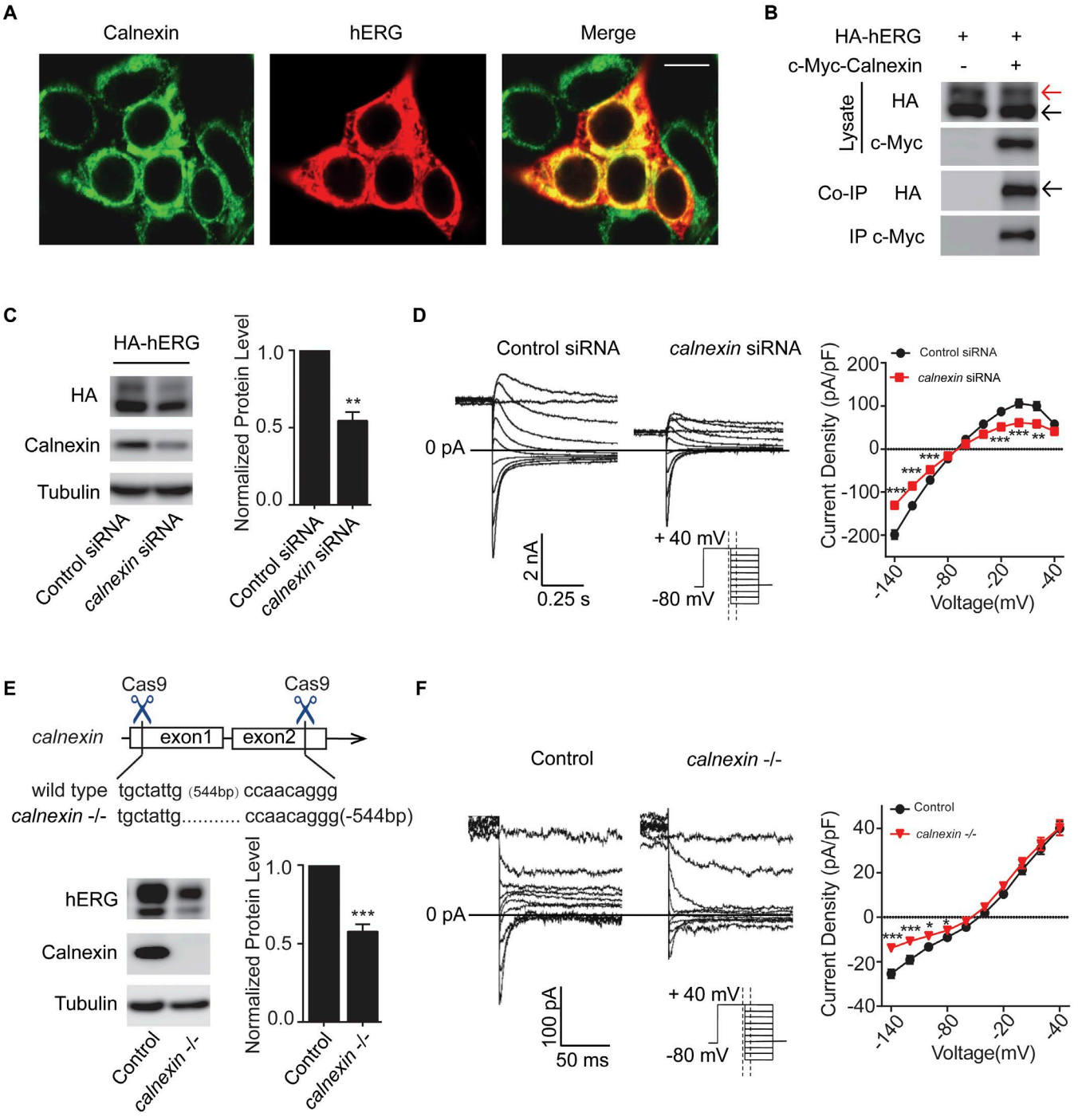

Figure 7. **Calnexin regulates the biogenesis of hERG proteins in mammalian cells. (A)** Localization of Calnexin and hERG expressed in HEK293T cells. hERG and Calnexin were detected using anti–HA and anti–Calnexin antibodies, respectively. Bar, 10 µm. **(B)** Coimmunoprecipitation of hERG with Calnexin expressed in HEK293T cells. Proteins were expressed in HEK293T cells and immunoprecipitated with anti–c-Myc antibody. The ER (~135 kD) and post-ER (~155 kD) forms of hERG proteins are indicated by black and red arrows, respectively. **(C)** Western blot analysis of hERG proteins in HEK293T cells treated with control siRNA or siRNAs targeting *calnexin*. **(D)** Representative traces (left) and current density (right) of hERG channels in HEK293T cells treated with control siRNA (n = 35) or siRNAs targeting *calnexin* (n = 33). **(E)** Western blots of endogenous hERG proteins in wild-type (control) and *calnexin* knockout (*calnexin*$^{-/-}$) SH-SY5Y cells. The deleted fragment (from 53 to 597 bp) of *calnexin* DNA in *calnexin*$^{-/-}$ cells is indicated. **(F)** Representative traces (left) and current density (right) of hERG channels in control (n = 26) and *calnexin*$^{-/-}$ (n = 20) SH-SY5Y cells. For D and F, the voltage protocols are shown under traces. All experiments were performed at least three times. *, P < 0.05; **, P < 0.01; ***, P < 0.001 (t test).

and function of UNC-103 K^+ channels in *C. elegans*. Down-regulation of its human homologue, Calnexin, significantly decreased the protein level and current density of the hERG K^+ channel in human SH-SY5Y cells. Thus, our findings reveal an evolutionally conserved role of CNX-1/Calnexin in regulating ERG-type K^+ channels across species.

Calnexin has been shown to play an important role in the protein folding of many secreted proteins, including ion channels (Gong et al., 2006; Li et al., 2010), G protein–coupled receptors (Free et al., 2007; Markkanen and Petäjä-Repo, 2008; Noorwez et al., 2009), MHC class I molecules (Ireland et al., 2007), and the nicotinic acetylcholine receptor (Chang et al., 1997). It has been also suggested that Calnexin facilitates the assembly of channel subunits into a stable complex (Chang et al., 1997; Green, 1999), but so far, there is no direct experimental evidence to support this idea. In this study, our findings show that CNX-1 facilitates biogenesis of ERG K^+ channels in *C. elegans* and promotes tetrameric assembly of ERG K^+ channels in a cell-free translation system, providing direct evidence to support this notion. However, the detailed mechanism underlying how Calnexin facilitates the biogenesis of ERG K^+ channels remains to be further studied.

Two major subtypes of chaperones exist in the ER: classical HSP family chaperones and carbohydrate-binding chaperones (Braakman and Hebert, 2013). It is generally thought that these two different types of chaperones cooperate during protein biogenesis to ensure adequate protein flux through the ER (Braakman and Hebert, 2013), but how they work together to control protein biogenesis remains largely unknown. Here, we demonstrate that two types of ER-located chaperones, Calnexin and J-proteins, facilitate the biogenesis of ion channels via distinct mechanisms, providing new insight into the role of ER-located chaperones in protein homeostasis.

The biogenesis of ion channels in the ER involves several steps, including glycosylation, folding, assembly, quality control, and ER exit. Besides Calnexin and DNAJB12/DNAJB14, some other chaperone proteins, including HSP70/HSC70 (Li et al., 2011), HSP90 (Ficker et al., 2003), DNAJA1/DNAJA2 (Walker et al., 2010), sig1R (Crottès et al., 2011), and FKBP38 (Walker et al., 2007) have been reported to be involved in the quality control, ER exit, or degradation of hERG. These chaperones may act at different stages of ERG channel biogenesis with distinct molecular mechanisms. This notion was supported by the findings that DNJ-1 and CNX-1 act in parallel to regulate the biogenesis of ERG K^+ channels, and previous studies have reported that different trafficking-defective hERG mutants show abnormal binding with different chaperones (Delisle et al., 2004; Curran and Mohler, 2015). Further dissection of the role of chaperones in ion channel biogenesis will facilitate our understanding of the channelopathies caused by defective biogenesis of ion channels.

Acknowledgments

We thank Mr. Cheng-Song Yan in Dr. Chen-Qi Xu's laboratory for helping us prepare liposomes and the *C. elegans* Genetics Center (funded by National Institutes of Health Office of Research Infrastructure Programs grant P40 OD010440) for providing worm strains.

This work was supported by the National Natural Science Foundation of China (grants 31471149 and 81527901).

The authors declare no competing financial interests.

Author contributions: X. Bai and K. Li performed most of the experiments. L. Yao and X.-L. Kang did the genetic screen. X. Bai generated transgenic worms and performed behavioral assays in these worm strains. K. Li cultured worm neurons and performed the electrophysiological recordings in worm neurons and mammalian cells. X. Bai cultured mammalian cells, performed genome editing in SH-SY5Y cells, and performed the immunoblot and immunocytochemistry experiments. X. Bai, K. Li, and S.-Q. Cai designed the study, analyzed data, and wrote the manuscript.

Sharona E. Gordon served as editor.

Submitted: 12 February 2018
Accepted: 15 May 2018

References

Anderson, C.L., B.P. Delisle, B.D. Anson, J.A. Kilby, M.L. Will, D.J. Tester, Q. Gong, Z. Zhou, M.J. Ackerman, and C.T. January. 2006. Most LQT2 mutations reduce Kv11.1 (hERG) current by a class 2 (trafficking-deficient) mechanism. *Circulation.* 113:365–373. https://doi.org/10.1161/CIRCULATIONAHA.105.570200

Anderson, C.L., C.E. Kuzmicki, R.R. Childs, C.J. Hintz, B.P. Delisle, and C.T. January. 2014. Large-scale mutational analysis of Kv11.1 reveals molecular insights into type 2 long QT syndrome. *Nat. Commun.* 5:5535. https://doi.org/10.1038/ncomms6535

Braakman, I., and D.N. Hebert. 2013. Protein folding in the endoplasmic reticulum. *Cold Spring Harb. Perspect. Biol.* 5:a013201. https://doi.org/10.1101/cshperspect.a013201

Chang, W., M.S. Gelman, and J.M. Prives. 1997. Calnexin-dependent enhancement of nicotinic acetylcholine receptor assembly and surface expression. *J. Biol. Chem.* 272:28925–28932. https://doi.org/10.1074/jbc.272.46.28925

Collins, K.M., and M.R. Koelle. 2013. Postsynaptic ERG potassium channels limit muscle excitability to allow distinct egg-laying behavior states in Caenorhabditis elegans. *J. Neurosci.* 33:761–775. https://doi.org/10.1523/JNEUROSCI.3896-12.2013

Crottès, D., S. Martial, R. Rapetti-Mauss, D.F. Pisani, C. Loriol, B. Pellissier, P. Martin, E. Chevet, F. Borgese, and O. Soriani. 2011. Sig1R protein regulates hERG channel expression through a post-translational mechanism in leukemic cells. *J. Biol. Chem.* 286:27947–27958. https://doi.org/10.1074/jbc.M111.226738

Curran, J., and P.J. Mohler. 2015. Alternative paradigms for ion channelopathies: disorders of ion channel membrane trafficking and posttranslational modification. *Annu. Rev. Physiol.* 77:505–524. https://doi.org/10.1146/annurev-physiol-021014-071838

Curran, M.E., I. Splawski, K.W. Timothy, G.M. Vincent, E.D. Green, and M.T. Keating. 1995. A molecular basis for cardiac arrhythmia: HERG mutations cause long QT syndrome. *Cell.* 80:795–803. https://doi.org/10.1016/0092-8674(95)90358-5

Davis, M.W., M. Hammarlund, T. Harrach, P. Hullett, S. Olsen, and E.M. Jorgensen. 2005. Rapid single nucleotide polymorphism mapping in C. elegans. *BMC Genomics.* 6:118. https://doi.org/10.1186/1471-2164-6-118

Delisle, B.P., B.D. Anson, S. Rajamani, and C.T. January. 2004. Biology of cardiac arrhythmias: ion channel protein trafficking. *Circ. Res.* 94:1418–1428. https://doi.org/10.1161/01.RES.0000128561.28701.ea

Doitsidou, M., R.J. Poole, S. Sarin, H. Bigelow, and O. Hobert. 2010. C. elegans mutant identification with a one-step whole-genome-sequencing and SNP mapping strategy. *PLoS One.* 5:e15435. https://doi.org/10.1371/journal.pone.0015435

Doyle, D.A., J. Morais Cabral, R.A. Pfuetzner, A. Kuo, J.M. Gulbis, S.L. Cohen, B.T. Chait, and R. MacKinnon. 1998. The structure of the potassium channel: molecular basis of K+ conduction and selectivity. *Science.* 280:69–77. https://doi.org/10.1126/science.280.5360.69

Ficker, E., A.T. Dennis, L. Wang, and A.M. Brown. 2003. Role of the cytosolic chaperones Hsp70 and Hsp90 in maturation of the cardiac potassium channel HERG. *Circ. Res.* 92:e87–e100. https://doi.org/10.1161/01.RES.0000079028.31393.15

Free, R.B., L.A. Hazelwood, D.M. Cabrera, H.N. Spalding, Y. Namkung, M.L. Rankin, and D.R. Sibley. 2007. D1 and D2 dopamine receptor expression is regulated by direct interaction with the chaperone protein calnexin. *J. Biol. Chem.* 282:21285–21300. https://doi.org/10.1074/jbc.M701555200

Garcia, L.R., and P.W. Sternberg. 2003. Caenorhabditis elegans UNC-103 ERG-like potassium channel regulates contractile behaviors of sex muscles in males before and during mating. *J. Neurosci.* 23:2696–2705. https://doi.org/10.1523/JNEUROSCI.23-07-02696.2003

Gong, Q., M.A. Jones, and Z. Zhou. 2006. Mechanisms of pharmacological rescue of trafficking-defective hERG mutant channels in human long QT syndrome. *J. Biol. Chem.* 281:4069–4074. https://doi.org/10.1074/jbc.M511765200

Goren, M.A., A. Nozawa, S.-i. Makino, R.L. Wrobel, and B.G. Fox. 2009. Cell-free translation of integral membrane proteins into unilamelar liposomes. *Methods Enzymol.* 463:647–673.

Green, W.N. 1999. Ion channel assembly: Creating structures that function. *J. Gen. Physiol.* 113:163–170. https://doi.org/10.1085/jgp.113.2.163

Harkcom, W.T., and G.W. Abbott. 2010. Emerging concepts in the pharmacogenomics of arrhythmias: ion channel trafficking. *Expert Rev. Cardiovasc. Ther.* 8:1161–1173. https://doi.org/10.1586/erc.10.89

Huffaker, S.J., J. Chen, K.K. Nicodemus, F. Sambataro, F. Yang, V. Mattay, B.K. Lipska, T.M. Hyde, J. Song, D. Rujescu, et al. 2009. A primate-specific, brain isoform of KCNH2 affects cortical physiology, cognition, neuronal repolarization and risk of schizophrenia. *Nat. Med.* 15:509–518. https://doi.org/10.1038/nm.1962

Ireland, B.S., M. Niggemann, and D.B. Williams. 2007. In Vitro Assays of the Functions of Calnexin and Calreticulin, Lectin Chaperones of the Endoplasmic Reticulum. *Methods Mol. Biol.* 347:331–342.

Isacoff, E.Y., L.Y. Jan, and D.L. Minor Jr. 2013. Conduits of life's spark: a perspective on ion channel research since the birth of neuron. *Neuron.* 80:658–674. https://doi.org/10.1016/j.neuron.2013.10.040

Johnson, J.N., N. Hofman, C.M. Haglund, G.D. Cascino, A.A.M. Wilde, and M.J. Ackerman. 2009. Identification of a possible pathogenic link between congenital long QT syndrome and epilepsy. *Neurology.* 72:224–231. https://doi.org/10.1212/01.wnl.0000335760.02995.ca

Li, K., Q. Jiang, X. Bai, Y.-F. Yang, M.-Y. Ruan, and S.-Q. Cai. 2017. Tetrameric Assembly of K^+ Channels Requires ER-Located Chaperone Proteins. *Mol. Cell.* 65:52–65. https://doi.org/10.1016/j.molcel.2016.10.027

Li, P., H. Ninomiya, Y. Kurata, M. Kato, J. Miake, Y. Yamamoto, O. Igawa, A. Nakai, K. Higaki, F. Toyoda, et al. 2011. Reciprocal control of hERG stability by Hsp70 and Hsc70 with implication for restoration of LQT2 mutant stability. *Circ. Res.* 108:458–468. https://doi.org/10.1161/CIRCRESAHA.110.227835

Li, Q., Y.-Y. Su, H. Wang, L. Li, Q. Wang, and L. Bao. 2010. Transmembrane segments prevent surface expression of sodium channel Nav1.8 and promote calnexin-dependent channel degradation. *J. Biol. Chem.* 285:32977–32987. https://doi.org/10.1074/jbc.M110.143024

Markkanen, P.M.H., and U.E. Petäjä-Repo. 2008. N-glycan-mediated quality control in the endoplasmic reticulum is required for the expression of correctly folded δ-opioid receptors at the cell surface. *J. Biol. Chem.* 283:29086–29098. https://doi.org/10.1074/jbc.M801880200

Meyer, R., and S.H. Heinemann. 1998. Characterization of an eag-like potassium channel in human neuroblastoma cells. *J. Physiol.* 508:49–56. https://doi.org/10.1111/j.1469-7793.1998.049br.x

Noorwez, S.M., R.R.K. Sama, and S. Kaushal. 2009. Calnexin improves the folding efficiency of mutant rhodopsin in the presence of pharmacological chaperone 11-cis-retinal. *J. Biol. Chem.* 284:33333–33342. https://doi.org/10.1074/jbc.M109.043364

Pardo, L.A., and W. Stühmer. 2014. The roles of K(+) channels in cancer. *Nat. Rev. Cancer.* 14:39–48. https://doi.org/10.1038/nrc3635

Petersen, C.I., T.R. McFarland, S.Z. Stepanovic, P. Yang, D.J. Reiner, K. Hayashi, A.L. George, D.M. Roden, J.H. Thomas, and J.R. Balser. 2004. In vivo identification of genes that modify ether-a-go-go-related gene activity in Caenorhabditis elegans may also affect human cardiac arrhythmia. *Proc. Natl. Acad. Sci. USA.* 101:11773–11778. https://doi.org/10.1073/pnas.0306005101

Ran, F.A., P.D. Hsu, J. Wright, V. Agarwala, D.A. Scott, and F. Zhang. 2013. Genome engineering using the CRISPR-Cas9 system. *Nat. Protoc.* 8:2281–2308. https://doi.org/10.1038/nprot.2013.143

Reiner, D.J., D. Weinshenker, H. Tian, J.H. Thomas, K. Nishiwaki, J. Miwa, T. Gruninger, B. Leboeuf, and L.R. Garcia. 2006. Behavioral genetics of caenorhabditis elegans unc-103-encoded erg-like K(+) channel. *J. Neurogenet.* 20:41–66. https://doi.org/10.1080/01677060600788826

Sanguinetti, M.C., C. Jiang, M.E. Curran, and M.T. Keating. 1995. A mechanistic link between an inherited and an acquired cardiac arrhythmia: HERG encodes the IKr potassium channel. *Cell.* 81:299–307. https://doi.org/10.1016/0092-8674(95)90340-2

Schrag, J.D., J.J.M. Bergeron, Y. Li, S. Borisova, M. Hahn, D.Y. Thomas, and M. Cygler. 2001. The Structure of calnexin, an ER chaperone involved in quality control of protein folding. *Mol. Cell.* 8:633–644. https://doi.org/10.1016/S1097-2765(01)00318-5

Strange, K., M. Christensen, and R. Morrison. 2007. Primary culture of Caenorhabditis elegans developing embryo cells for electrophysiological, cell biological and molecular studies. *Nat. Protoc.* 2:1003–1012. https://doi.org/10.1038/nprot.2007.143

Swanton, E., S. High, and P. Woodman. 2003. Role of calnexin in the glycan-independent quality control of proteolipid protein. *EMBO J.* 22:2948–2958. https://doi.org/10.1093/emboj/cdg300

Taglialatela, M., A. Pannaccione, P. Castaldo, G. Giorgio, Z. Zhou, C.T. January, A. Genovese, G. Marone, and L. Annunziato. 1998. Molecular basis for the lack of HERG K+ channel block-related cardiotoxicity by the H1 receptor blocker cetirizine compared with other second-generation antihistamines. *Mol. Pharmacol.* 54:113–121. https://doi.org/10.1124/mol.54.1.113

Trudeau, M.C., J.W. Warmke, B. Ganetzky, and G.A. Robertson. 1995. HERG, a human inward rectifier in the voltage-gated potassium channel family. *Science.* 269:92–95. https://doi.org/10.1126/science.7604285

Vandenberg, J.I., M.D. Perry, M.J. Perrin, S.A. Mann, Y. Ke, and A.P. Hill. 2012. hERG K(+) channels: structure, function, and clinical significance. *Physiol. Rev.* 92:1393–1478. https://doi.org/10.1152/physrev.00036.2011

Walker, V.E., R. Atanasiu, H. Lam, and A. Shrier. 2007. Co-chaperone FKBP38 promotes HERG trafficking. *J. Biol. Chem.* 282:23509–23516. https://doi.org/10.1074/jbc.M701006200

Walker, V.E., M.J. Wong, R. Atanasiu, C. Hantouche, J.C. Young, and A. Shrier. 2010. Hsp40 chaperones promote degradation of the HERG potassium channel. *J. Biol. Chem.* 285:3319–3329. https://doi.org/10.1074/jbc.M109.024000

Ware, E., F.A. Vassilakos, P. Peterson, M.R. Jackson, M.A. Lehrman, and D.B. Williams. 1995. The molecular chaperone calnexin binds Glc1Man9GlcNAc2 oligosaccharide as an initial step in recognizing unfolded glycoproteins. *J. Biol. Chem.* 270:4697–4704.

Zhou, Z., Q. Gong, B. Ye, Z. Fan, J.C. Makielski, G.A. Robertson, and C.T. January. 1998. Properties of HERG channels stably expressed in HEK 293 cells studied at physiological temperature. *Biophys. J.* 74:230–241. https://doi.org/10.1016/S0006-3495(98)77782-3